

Sensor R&D for the CMS outer tracker upgrade for the HL-LHC

This content has been downloaded from IOPscience. Please scroll down to see the full text.

2014 JINST 9 C04033

(<http://iopscience.iop.org/1748-0221/9/04/C04033>)

View [the table of contents for this issue](#), or go to the [journal homepage](#) for more

Download details:

IP Address: 188.184.3.56

This content was downloaded on 15/06/2015 at 11:08

Please note that [terms and conditions apply](#).

13th TOPICAL SEMINAR ON INNOVATIVE PARTICLE AND RADIATION DETECTORS
7–10 OCTOBER 2013
SIENA, ITALY

Sensor R&D for the CMS outer tracker upgrade for the HL-LHC

H. Behnamian¹

*Institute for Research in Fundamental Sciences (IPM),
Tehran, Iran*

E-mail: hadi.behnamian@cern.ch

ABSTRACT: At an instantaneous luminosity of $5 \times 10^{34} \text{ cm}^{-2} \text{ s}^{-1}$, the high-luminosity phase of the Large Hadron Collider (HL-LHC) is expected to deliver a total of 3000 fb^{-1} of collisions, hereby increasing the discovery potential of the LHC experiments significantly. However, the radiation environment of the tracking system will be severe, requiring new radiation hard sensors for the CMS tracker. The CMS tracker collaboration has almost completed a large material investigation and irradiation campaign to identify the silicon material and design that fulfills all requirements of a new tracking detector at HL-LHC. Focusing on the upgrade of the outer tracker region, pad diodes as well as fully functional strip sensors have been implemented on silicon wafers with different material properties and thicknesses. The samples were irradiated with a mixture of neutrons and protons corresponding to fluences as expected for various positions in the future tracker. The measurements performed on the structures include electrical sensor characterization, measurements of the collected charge and bulk defect characterization. In this paper, the performance and limitations of the different materials are presented.

KEYWORDS: Radiation-hard detectors; Solid state detectors; Particle tracking detectors (Solid-state detectors)

¹On behalf of the CMS Tracker Collaboration.

Contents

1	Introduction	1
2	Measurement campaign overview	2
2.1	The wafer and materials	2
2.2	Irradiation	4
3	Measurement setup and results	5
3.1	Charge collection	5
3.2	Study of random ghost hits	7
3.3	Device simulation	10
4	Summary and outlook	11

1 Introduction

The upgrade of the Large Hadron Collider (LHC), known as the High Luminosity-LHC [1], is scheduled for 2022. After the upgrade, LHC has planned to deliver an integrated luminosity of up to 3000 fb^{-1} . In these conditions, events will feature a higher quantity of tracks in the detector volume and there will be a much harsher radiation environment, with respect to current LHC operations. From simulations of the radiation environment at the Compact Muon Solenoid experiment (CMS), one expects a maximum particle fluence of $1.5 \times 10^{15} \text{ n}_{\text{eq}}/\text{cm}^2$ for the silicon strip tracker regions (shown in figure 1). Hence it is required to install a new tracker detector, built with a material able to withstand the radiation rate, and a layout that guarantees a granularity higher than the actual CMS tracker one.

The CMS Tracker Collaboration has ordered a large number of 6 inch wafers to the producer Hamamatsu Photonics K. K. (HPK)¹ to investigate possible sensor technologies and materials. To identify the future silicon sensor technology baseline for the phase II upgrade of tracker, CMS started a so called HPK measurement campaign. To find radiation hard materials, an extended mixed irradiation program with protons and neutrons has been set up for the materials of interest. These sensors have been irradiated to various fluences corresponding to the ones expected at different radii in the future tracker, searching for the best material, manufactured by a widely recognised producer.

¹<http://www.hamamatsu.com>.

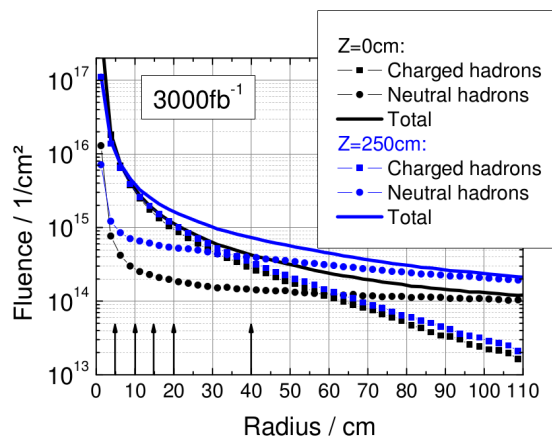


Figure 1. Simulated fluences by FLUKA for the CMS tracker, as a function of the radius from the interaction point [2].

2 Measurement campaign overview

To investigate possible sensor technologies and materials, the CMS Tracker Collaboration has ordered a large number of 6 inch wafers from the producer HPK. These wafers were produced with different substrates, thicknesses, implants and geometries. Also concerning the radiation hard material, three different silicon growth techniques with various oxygen contents have been used.

2.1 The wafer and materials

The common wafer layout has been designed with a variety of structures. Each wafer contains many test structures used for different purposes (figure 2), some important parts of which are introduced below [3].

- **Diodes:** material properties and response to irradiation are investigated with different diodes. They are used to characterise the material through electric measurements (IV- and CV-curves) and dark current measurements for the detector are derived from the measurements on them.
- **Test Structures:** there are test structures to qualify and monitor the quality of the production process and determine operating parameters as well as mini sensors for beam tests and source measurements. These allow for the actual assembly of modules and therefore investigation of the influence of geometry and materials on resolution, noise and signal-to-noise ratio. Ten different measurements can be performed with this structure. The interstrip parameters (capacitance and resistance) and dielectric break down voltage are taken from test structures consisting of strips.
- **Baby sensors:** an idea to save material in the tracker is to implement the pitch adapter, used to connect to the readout with wirebonds, directly on the sensor. The standard baby sensors are produced by converting the about 80 μm pitch of the strips to about 45 μm pitch of the read-out chip pads [4]. These mini-strip sensors are used to evaluate radiation hardness of the different materials.

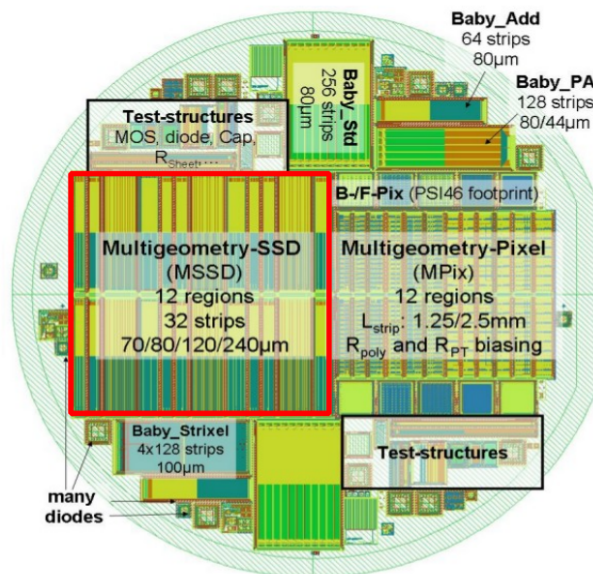


Figure 2. The HPK campaign wafer with the different structures.

- **Multi-Geometry Silicon-Strip Detector (MSSD):** this article focuses on the MSSD which are highlighted with a red square in figure 2. The MSSD structure was used for beam tests and measurements with radioactive sources. It contained 12 different regions with different strip pitches and width-to-pitch ratios. Strips are arranged in groups of 32 strips with different pitches from 70 to 240 μm . This kind of sensors could be used in the inner region of the Phase II strip tracker. These sensors allow for the actual assembly of modules and therefore for the investigation of the influence of geometry and materials on resolution, noise and signal-to-noise ratio. In this paper, charge collection and a new effect, namely random ghost hits, will be investigated.
- **Multi-geometry pixel sensors:** this structure is used for characterisation of a sensor with very short strips (1–2 mm), varying pitch and biasing connection (poly-silicon or punch-through). The main focus of multi-geometry pixel structures are the capacitance measurements, as they lead to conclusions on the noise behaviour. One possible solution to cope with the higher track density is the use of so called strixels, where the words strip and pixel are combined. These strixel sensors contain segmented strips with a larger area compared to the pixel detectors.

This layout with different active thicknesses has been processed by different technologies for the substrate production. It has been shown [5] that silicon substrates with a high oxygen content show a higher degree of radiation tolerance. Therefore this campaign features materials with different oxygen contents:

- **Float Zone (FZ):** the best known material which serves as a reference and has also a high quality in terms of the high resistance values.

- Magnetic Czochralski (MCZ): this growth technique results in a high oxygen content in the silicon, which was shown to be beneficial in terms of radiation hardness.
- Epitaxial (Epi): this method allows to produce very thin (25–100 μm) active sensors by chemical vapour deposition of silicon on a carrier wafer.

For each type, p-strip implant in n-bulk material (n-type) and n-strip in p-bulk (p-type) were produced. For the n-in-p sensors, to avoid low interstrip resistances due to inversion layers, two different strip isolation technologies are tested. The sensor types named with letter P (p-stop) use a p+ layer between the n+ strips to intercept the electron accumulation layer, whereas sensor types labelled with the letter Y (p-spray) introduce a p doping on the full surface. In addition, wafers with a second metallization layer were also produced to investigate the radiation hardness and the noise behaviour with directly connected electronics.

To investigate the properties of sensors we have ordered various thicknesses. The FZ material is available in 320 and 200 μm physical thickness, 120 μm on carrier wafer and 320 μm thick with a reduction of active thickness (to 200 and 120 μm) by deep diffusion of the backside doping. The MCZ material is physically 200 μm thick and the epitaxial wafers come in 50, 75 and 100 μm versions.

An advantage of thinner sensors is the lower depletion voltage compared to thicker sensors. After irradiation also trapping of charge carriers is reduced due to the reduced thickness and a higher electrical field. A reduction of the active thickness can be achieved with deep diffusion. The deep diffusion process allows to produce thin sensors at lower costs compared to the thinning process or wafer bonding. The active thickness is reduced but the physical thickness is still 320 μm , which allows easier handling than with thinner wafers, but a potential benefit for the material budget with thinner sensors would be abandoned. Labels for the materials for this paper are composed of silicon type (FZ; MCZ; FTH: thinned float zone), nominal active thickness (320, 200 μm) and doping type (N: n-bulk; P: p-bulk with p-stop; Y: p-bulk with p-spray).

2.2 Irradiation

The radial dependence of neutral and charged hadron fluences differs significantly (figure 1), which leads to a variation of the ratio of charged to neutral hadrons as a function of radius. It was found that neutrons, protons and mixed irradiations lead to different effects in different materials. Therefore we need to probe these effects on our materials in a consistent way. Since we cannot survey the conditions in the entire tracker volume, we picked some representative points as summarized in first two lines of table 1.

Several irradiation steps have already been carried out and different materials were irradiated with 1 MeV neutrons from the reactor in Ljubljana, Slovenia, and with 25 MeV protons from the cyclotron in Karlsruhe that are mainly funded by AIDA.² The annealing effects at room temperature due to the transport from the irradiation facilities to the individual institutes, where the measurements are performed, have to be considered.

²<http://aida.web.cern.ch/>.

Table 1. Summary of the foreseen particle fluences at $z = 250$ cm. The maximum fluences for the CMS sensors discussed in this paper correspond to $r = 20$ cm

Radius	Protons, $10^{14} n_{eq}/\text{cm}^2$	Neutrons, $10^{14} n_{eq}/\text{cm}^2$	Total, $10^{14} n_{eq}/\text{cm}^2$	Ratio p/n
40 cm	3	4	7	0.75
20 cm	10	5	15	2.0
15 cm	15	6	21	2.5
10 cm	30	7	37	4.3
5 cm	130	10	140	13

3 Measurement setup and results

Some strip properties like signal (charge collection) and noise were determined in laboratory measurements by using the CMS readout system. For testing purposes, the sensors were mounted on an aluminium plate and wire bonded to APV25 readout chips [6]. For the signal and noise measurements, these MSSD modules are exposed to particles from a radioactive beta source (^{90}Sr). In the next two sections, we will examine these measurements by varying bias voltage, fluence, annealing time and temperature for different geometries.

3.1 Charge collection

The signal to noise ratio is the most important parameter for hit identification. The collected charge was measured after irradiation with the beta source. To have a better statistical information on the collected charge, this procedure was performed for many times. These obtained distributions were fitted with convoluted Landau and Gaussian functions which reproduced the histograms very accurately. From the fit, the most probable value (MPV) was extracted and we'll name this parameter as cluster charge in the following figures. The CBC³ (CMS binary chip) [7] noise threshold is expected to be between 4000 and 6000 electrons, thus we consider 8000 electrons to be acceptable as signal. In this section, we present collected charge values at some fixed applied bias voltage as a function of fluence and annealing time for different materials.

Figure 3 shows the degradation of the collected charge for FZ320 μm materials at 600 V and 900 V reverse bias (n-bulk on the left and p-bulk on the right). These measurements have been done for different irradiations up to $1.5 \times 10^{15} n_{eq}/\text{cm}^2$, which is the highest expected fluence. The initially higher signal of the thick materials drops fast with increasing fluence. To make a comparison between CMS and ATLAS results, we put ATLAS results ([8] and [9]) into the same plot with equivalent doses of neutron and proton irradiations for both p and n-bulk materials separately.

In general, it has been found that for n-bulk materials (left side of figure 3), CMS measured higher signal than ATLAS but it must be noticed that the two experiments used sensors with different thicknesses. Also there are some differences between vendors⁴ and irradiation types (ATLAS results are obtained with only neutron irradiations while CMS used mixed ones). It is apparent that

³The existing CMS tracker readout chip (APV) uses analogue pipeline storage and readout. But at the HL-LHC, high speed off-detector digital links will be needed. To reach this goal, CMS uses digital readout chip with a comparator to select "hit" or "no hit" on each strip. The programmable threshold setting is one of advantages of this binary chip.

⁴ATLAS has tested materials produced by <http://www.micronsemiconductor.co.uk/>.

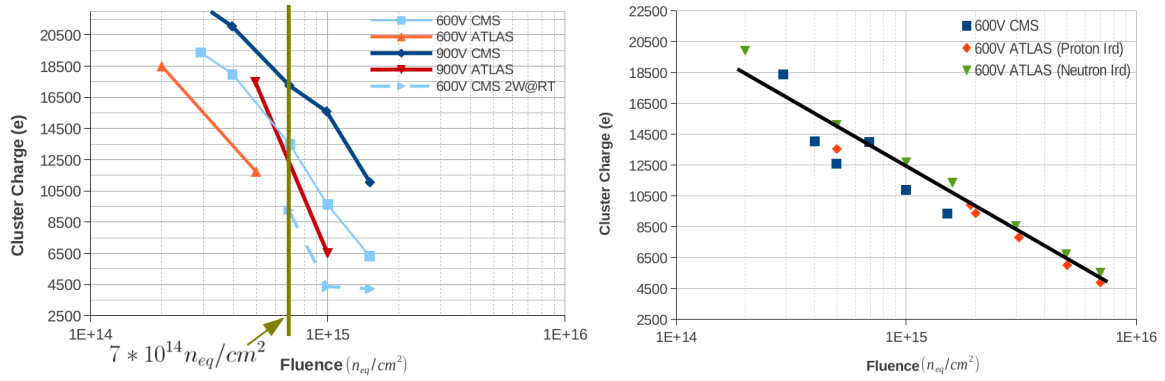


Figure 3. The collected charge vs. irradiation fluence for FZ320 μm (n-bulk on the left and p-bulk on the right). The ATLAS data were extracted from references [8, 9]. The CMS measurements [3] have been taken at -20°C with a ^{90}Sr beta source by using APV25 read-out system. A cluster has been defined so that a seed and neighbours signals are bigger than three and two times the strip noise, respectively.

n-bulk strip sensors could be used for fluences below $7 \times 10^{14} \text{ n}_{\text{eq}}/\text{cm}^2$, but above one can observe a strong decrease in cluster charge below the CBC threshold. Then this kind of sensors would not be useful for higher irradiation scenarios of phase II tracker upgrade.

In the case of FZ320 μm p-bulk material (right side of figure 3), the behaviour of collected charge after irradiation is consistent for all thick sensors. The cluster charge in this case shows a uniform drop trend. Our measurements on these strip sensors show a signal higher than 8000 electrons even after high irradiation fluences of $1 \times 10^{15} \text{ n}_{\text{eq}}/\text{cm}^2$. This level of signal-to-noise is sufficient for high signal efficiency and low noise occupancy. We define the seed signal equal to the sum of collected charge by strips which have signal to noise ratio bigger than three. The left part of figure 4 shows the seed signal for all thin materials with 200 μm thickness at fixed bias voltage of 600 V without any annealing. It seems for fluence below $7 \times 10^{14} \text{ n}_{\text{eq}}/\text{cm}^2$, n-bulk sensors have higher seed signals with respect to p-bulk ones. Then n-bulk strip sensors could still be used in this range of fluence. In the case of higher irradiation levels, the collected charge for n-bulk materials were not high enough to be taken into account as signal. The results of the comparison for the FZ material with different thicknesses (200 and 320 μm) are shown on the right side of figure 4. It can be seen that after higher fluence of $1 \times 10^{15} \text{ n}_{\text{eq}}/\text{cm}^2$, the physically thin materials collect comparable or even slightly more charge than the thick sensors. Thus 200 μm thick strip sensors allow to reduce the material budget and keep the charge collection at the same level as 320 μm thick sensors at high fluence.

One important parameter to study irradiated sensors is the annealing effect on charge collection. Figure 5 shows the dependence of the seed signal on annealing time at room temperature (RT), for fixed fluences and different materials and thicknesses. These two plots are related to medium fluence ($7 \times 10^{14} \text{ n}_{\text{eq}}/\text{cm}^2$) and high irradiation level ($1 \times 10^{15} \text{ n}_{\text{eq}}/\text{cm}^2$) for devices that were temperature annealed. For both of them, signal is more stable for p-bulk sensors than n-bulk ones. In the case of medium level, all thin p and n-bulk samples work well and show seed signals bigger than 8000 electrons even with high amount of annealing (20 weeks at room temperature). For high irradiation (right side of figure 5), signal on n-bulk sensor decreases after a few weeks at

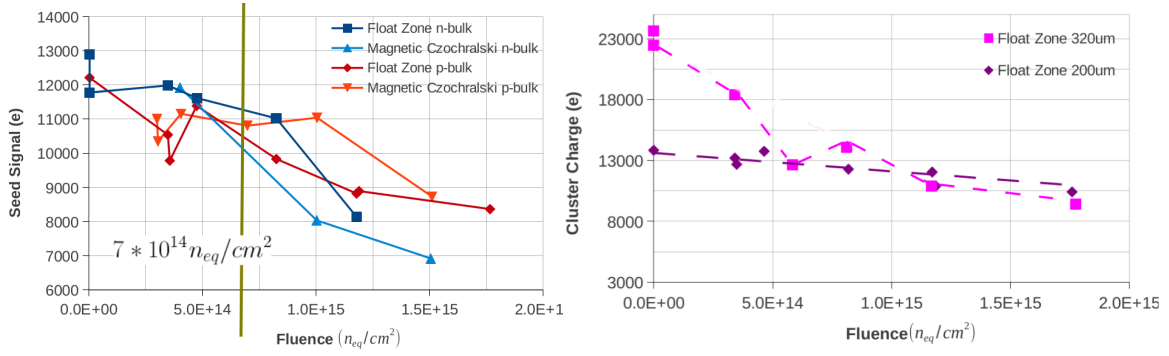


Figure 4. Left: seed signal vs. irradiation fluence for FZ200 μm p and n-bulk materials. Right: cluster charge comparison between thick (320 μm) and thin (200 μm) FZ sensors. Both of them are measured at fixed bias voltage of 600 V without any annealing.

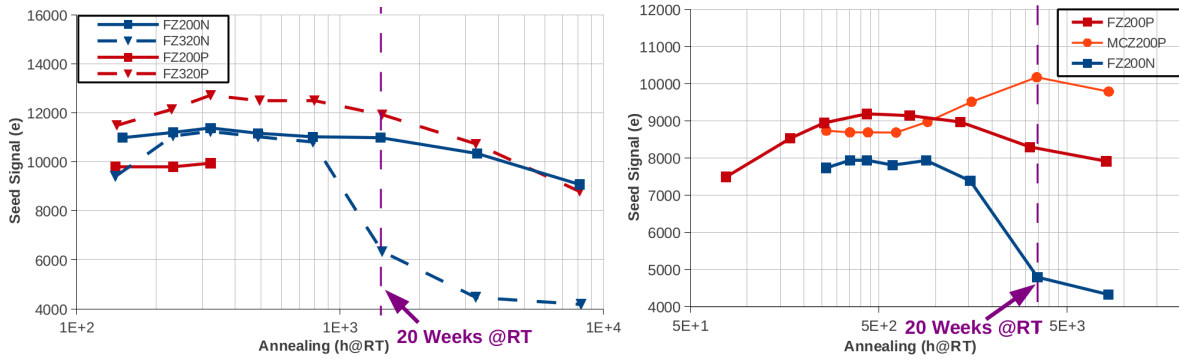


Figure 5. Annealing behaviour of seed signal at fixed bias voltage equals to 600 V for two different irradiation levels as a function of annealing time at room temperature. Left: medium fluence ($7 \times 10^{14} \text{ n}_{\text{eq}}/\text{cm}^2$) and Right: high fluence: ($1 \times 10^{15} \text{ n}_{\text{eq}}/\text{cm}^2$).

room temperature to a low level. This is one reason why p-bulk will be the best choice for the outer part of the tracker at the phase II upgrade project. This effect is also most pronounced for MCZ material, which also has a higher signal with annealing than FZ as shown at higher fluences.

3.2 Study of random ghost hits

High fluences could damage the sensors and increase their leakage current, the depletion voltage and charge carrier trapping. The higher leakage current causes higher noise and more heat load. Hence it is required to study the noise distributions of different materials at higher fluences. It is expected that the noise follows a Gaussian distribution before and after irradiation, but CMS has observed that the noise distributions have large non-Gaussian tails (see figure 6). These fake hits have been created especially for irradiated n-bulk sensors and they can lead to strip occupancies of more than 1% even if no particles are crossing the sensor. At low voltages the noise distribution is Gaussian while at high voltages significant noise tails may lead to noise hits. By taking noise measurements without particles crossing and fitting them with Gaussian function, we can define fake hits which exceed the threshold of 5σ . Then taking a signal run, in presence of particle

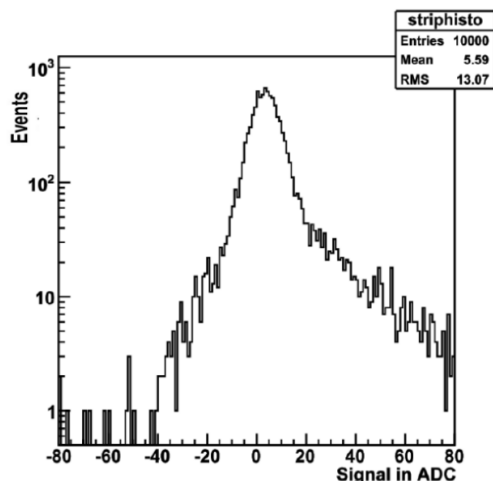


Figure 6. Example of pedestal-subtracted noise distribution in irradiated n-type strip sensors at 900 V taken from ref. [3].

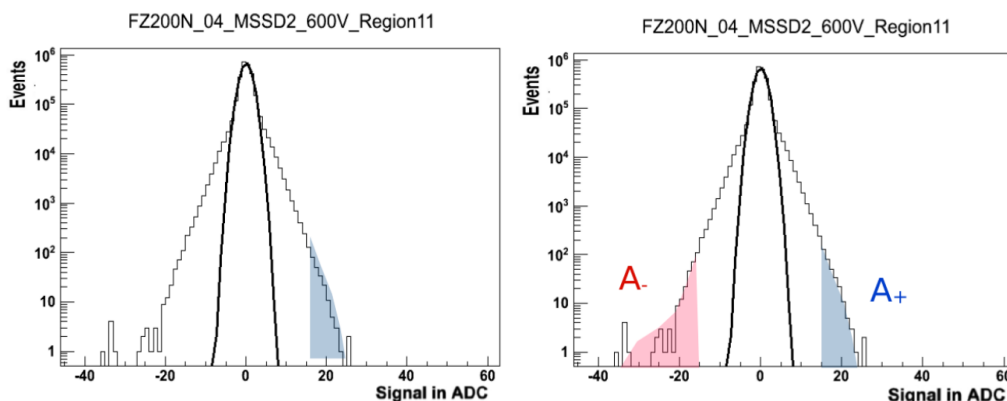


Figure 7. Two different definitions of the fake hits rate.

source, the experimental amount of signal which contains fake hit effects will be measured. We need more study on this new effect and finally choose the best material with lowest fake hits rate for the CMS tracker upgrade project. To compute fake hit rates, we defined two methods, as illustrated in figure 7. We extracted 5σ cuts by fitting noise distributions with Gaussian functions. In the first method, the strip occupancy is defined as the number of signals exceeding 5σ cuts at positive side band divided by the number of strips and the number of events (left plot at figure 7). In the second definition, we built fake hits as subtraction of signals exceeding 5σ cuts at two side bands divided by the number of strips and the number of events (right plot at figure 7). The strip occupancy due to non-Gaussian noise hits depends on bias voltage, fluence and annealing time. To study this effect we made a scan in the phase space of these parameters and extracted the fake hits rate.

Figure 8 shows the strip occupancy due to noise hits (by using the first method) as a two dimensional function of bias voltage and annealing time. It can be seen that no effect appeared in p-bulk sensors even after mixed irradiation (top-left part), while these measurements show visible

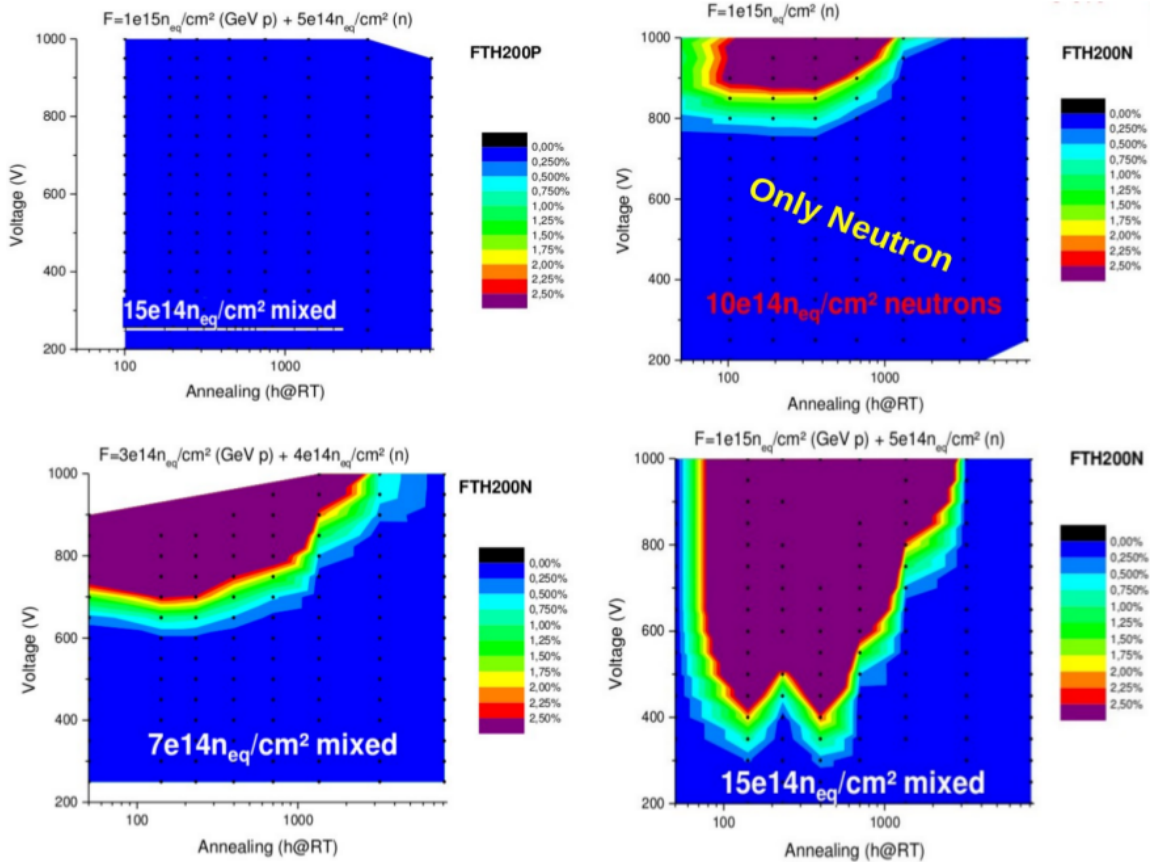


Figure 8. Strip occupancy due to random noise hits as a function of bias voltage and annealing time after irradiation (irradiation type and levels have been labelled on each plots). Top-left: p-bulk with mixed irradiation, Top-right: n-bulk with only neutron irradiation, Bottom: n-bulk with two different mixed irradiation levels.

effects for n-bulk materials for every irradiation type. Also after longer annealing of about 90 days, the rate of strip occupancy is going down again. In case of only neutron irradiated n-bulk sensors (top-right side), higher bias voltages of about 800 V are needed to produce fake hits. This effect is less pronounced for neutron irradiation compared to irradiation with charged hadrons (see bottom side of figure 8). For higher mixed irradiation levels, this effect starts even at low voltages of about 300 V. This difference of charged and neutral hadron irradiations indicates that ionising energy loss in the SiO_2 interface might be relevant. This dependence on the type of ionizing radiation hints towards a combined effect of bulk damage and surface charge. The simulation of surface and bulk damages can help to study this effect in more detail.

Before studying the simulation of this effect, we have investigated fake hit contributions for different geometries (different strip width and pitches). To study random ghost hits on different geometries we used MSSD with 12 regions depicted on the left side of figure 9. We measured the voltage for which the random ghost hits appeared (called turn-on voltage) for all of the materials in different regions. It can be noticed that the second definition of fake hits rate was assumed for this study. Figure 9 shows the turn-on voltage for a variety of materials at different irradiation levels

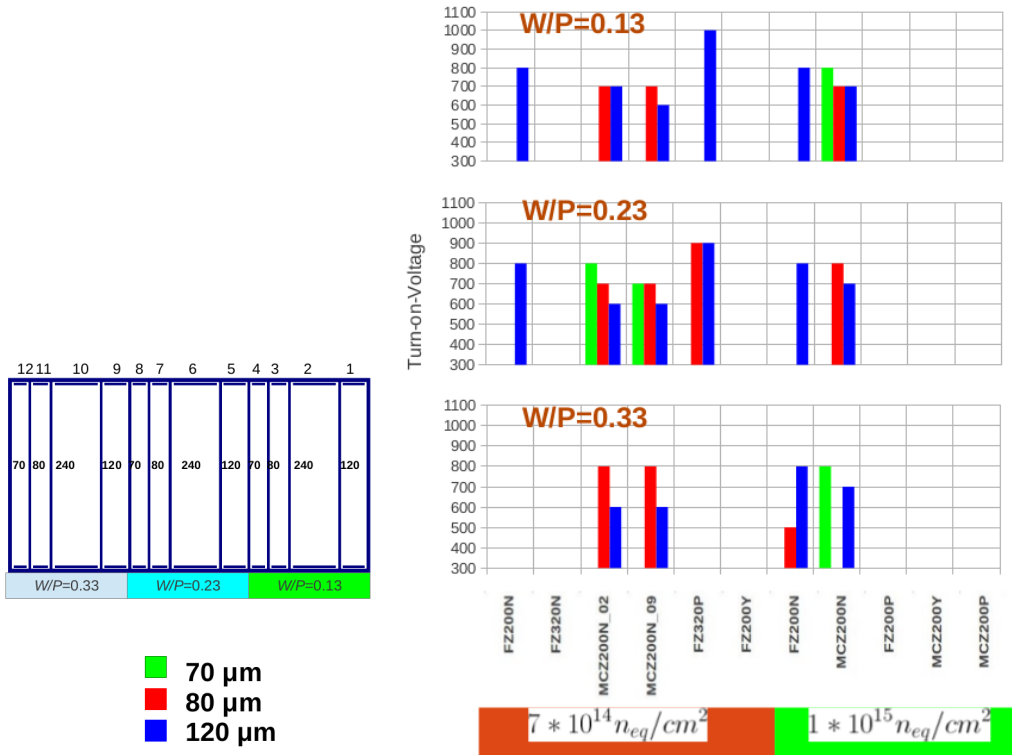


Figure 9. Left: feature of MSSD with 12 regions. Every region has a specific combination of strip width and pitch, and is shown with different color labels. Right: turn-on-voltage for present materials with different fluence, strip width and width-to-pitch ratios.

with different strip width and pitches. It can be seen that this effect has not appeared for p-bulk sensors with 200 μm thicknesses even at higher bias voltage. The other consequence is that regions with high strip pitches are affected earlier.

3.3 Device simulation

To investigate the random ghost hits, the device was simulated. Although the main reason of this effect is still under study, it can be shown that there are some correlations between fake hits results and the simulation of electric field intensity below the SiO_2 layer. First simulations which take into account both the bulk defects generated by non-ionising energy loss and the increased oxide charge density due to ionising energy loss show very high electric fields close to the p+ strip implants for n-type sensors. An oxide charge density of $1.2 \times 10^{12} \text{ cm}^{-2}$ is assumed and bulk defects are implemented which correspond to a fluence of $1 \times 10^{15} \text{ n}_{eq}/\text{cm}^2$. The electric field intensity at 0.1 μm below the SiO_2 layer is shown on the left side of figure 10. This is the first correlation between simulation and measurements, because as mentioned earlier only for n-bulk materials the fake hits effect was observed. Simulations show higher electric fields at the strip edges for irradiated n-bulk while no field peaks are seen for p-bulk materials. Notice that lowering the values used for oxide charge concentration decreases the peak value of the electric field in n-type sensors (middle plot of figure 10). And this would explain why random ghost hits are reduced for only neutron irradiation with less ionization (second correlation). As shown in figure 9, regions

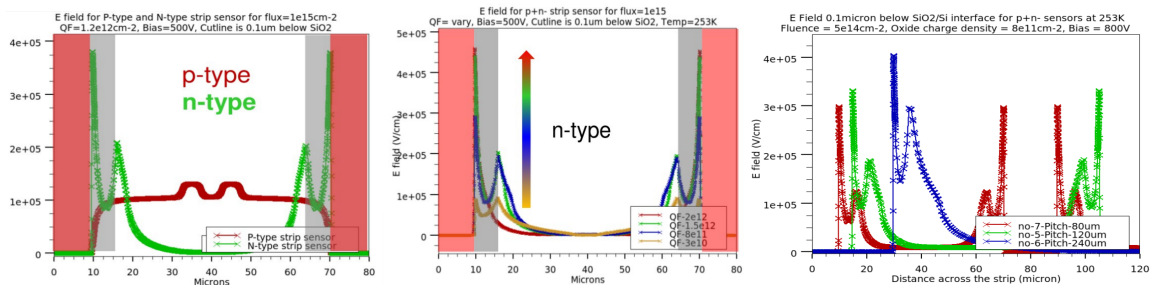


Figure 10. Electric field intensity simulation at $0.1 \mu\text{m}$ below the SiO_2 layer (see ref. [10]).

with high strip pitches are affected earlier. This could be confirmed with simulation as shown on the right side of figure 10. From simulation, it is apparent that these regions have higher electric field peaks than others (third correlation).

4 Summary and outlook

To find the best choice material for CMS outer tracker at high luminosity LHC, signal and noise were studied on sensors produced within the HPK campaign. To reach this goal, sensors were irradiated to fluences expected at radii of 20 and 40 cm. The output of the measurements can be summarized as follows:

- n-bulk vs. p-bulk materials: for medium irradiation, n-bulk materials give higher signals, but at higher fluences the p-bulk sensors collect more charge carriers. Signal on n-bulk materials is decreased after a couple of weeks at room temperature while charge collection is rather stable for p-bulk sensors. Also as we mentioned for n-bulk, fake hits are created and increase the strip occupancy. This new effect could be explained with the simulation of the electric field of the device and needs to be studied further.
- FZ vs. MCZ: sensors made of MCZ silicon show an increased signal with annealing. Operation of MCZ sensors would enable annealing scenarios with longer annealing times and hence with lower dark current, less power consumption and lower heat generation.
- 200 vs. 320 μm thickness: the collected charge was comparable for both of them especially for sensors that will be located at a radius of 20 cm. Thinner strip sensors allow to reduce the material budget and keep the charge collection at the same level as 320 μm thick sensors especially at high fluences.

Finally due to the good charge collection performance of the p-bulk materials after irradiation with the expected fluences, and since non-Gaussian noise hits were not observed for them, CMS decided to use p-bulk sensors for the tracker and concentrate the future work on optimizing the technology and the geometry.

Acknowledgments

The research leading to these results has received funding from the European Commission under the FP7 Research Infrastructures project AIDA, grant agreement no. 262025.

References

- [1] F. Gianotti et al., *Physics potential and experimental challenges of the LHC luminosity upgrade*, *Eur. Phys. J. C* **39** (2005) 293 [[hep-ph/0204087](#)].
- [2] S. Muller, *The Beam Condition Monitor and the Radiation Environment of the CMS Detector at the LHC*, Karlsruhe Institute of Technology, IEKP-KA/2011-1, CMS TS-2010/042 (2011).
- [3] A. Dierlamm, *Characterisation of silicon sensor materials and designs for the CMS Tracker Upgrade* [PoS\(Vertex 2012\)016](#).
- [4] CMS TRACKER collaboration, A. Dierlamm, *Silicon sensor developments for the CMS tracker upgrade*, [2012 JINST 7 C01110](#).
- [5] CERN RD50 collaboration, M. Moll et al., *Development of radiation tolerant semiconductor detectors for the Super-LHC*, *Nucl. Instrum. Meth. A* **546** (2005) 99.
- [6] M. Raymond et al., *The CMS Tracker APV25 0.25 μm CMOS Readout Chip*, presented at *Sixth Workshop on Electronics for LHC Experiments*, CERN/LHCC/2000-041 (2000).
- [7] W. Ferguson et al., *The CBC microstrip readout chip for CMS at the high luminosity LHC*, [2012 JINST 7 C08006](#) [[INSPIRE](#)].
- [8] G. Casse et al., *Measurements of charge collection efficiency with microstrip detectors made on various substrates after irradiations with neutrons and protons with different energies*, [PoS\(VERTEX 2008\)036](#).
- [9] G. Casse et al., *Evidence of enhanced signal response at high bias voltages in planar silicon detectors irradiated up to 2.2×10^{16} $\text{n}_{\text{eq}}/\text{cm}^2$* , *Nucl. Instrum. Meth. A* **636** (2011) S56.
- [10] R. Ranjeet et al., *Simulations for Hadron Irradiated n+p- Si Strip Sensors Incorporating Bulk and Surface Damage*, presented at *23rd RD50 Workshop*, CERN, Switzerland (2013).